

COURLIS

Validation Manual

Version v8p5
December 1, 2023



Contents

1	Canal equilibre	5
1.1	Purpose	5
1.2	Description	5
1.2.1	Physical parameters	5
1.2.2	Numerical parameters	6
1.3	Results	6
1.4	Conclusion	7
2	Newton	9
2.1	Purpose	9
2.2	Description	9
2.3	Physical parameters	10
2.4	Numerical parameters	10
2.5	Results	11
2.6	Conclusion	11
3	Newton trapeze	13
3.1	Purpose	13
3.2	Description	13
3.2.1	Construction of a trapezoidal channel	13
3.2.2	Parameters	14
3.3	Results	14
3.4	Conclusion	15
4	Soni	18
4.1	Purpose	18
4.2	Description	18
4.3	Physical parameters	19

4.4	Numerical parameters	19
4.5	Results	19
4.6	Conclusion	19
5	Soni trapeze	22
5.1	Purpose	22
5.2	Description	22
5.3	Results	22
5.4	Conclusion	22
6	Van Rijn	26
6.1	Purpose	26
6.2	Description	26
6.3	Physical parameters	26
6.4	Numerical parameters	26
6.5	Results	26
6.6	Conclusion	26
7	Bedload formulae test	29
7.1	Purpose	29
7.2	Description	29
7.2.1	Physical parameters	29
7.2.2	Numerical parameters	29
7.3	Results	29
7.4	Conclusion	29
8	Cohesive channel	31
8.1	Erosion	31
8.1.1	Purpose	31
8.1.2	Description	31
8.1.3	Physical parameters	31
8.1.4	Analytical solution	32
8.1.5	Numerical parameters	32
8.1.6	Results	32
8.1.7	Conclusion	32
8.2	Deposition	32
8.2.1	Purpose	32
8.2.2	Description	33
8.2.3	Physical parameters	33
8.2.4	Analytical solution	34
8.2.5	Numerical parameters	35
8.2.6	Results	35

8.2.7	Conclusion	35
9	Dambreak	37
9.1	Purpose	37
9.2	Description	37
9.2.1	Physical parameters	37
9.2.2	Numerical parameters	38
9.3	Results	38
9.4	Conclusion	38
	Bibliography	39

1. Canal equilibre

1.1 Purpose

This test computes the bedload for an equilibrium channel.

1.2 Description

1.2.1 Physical parameters

The steady state is obtained from the equilibrium between the slope and the friction term,

$$gR_h \partial_x z_b = \frac{\tau}{\rho}, \quad (1.1)$$

with the shear stress τ defined by,

$$\tau = \rho g R_h \frac{u|u|}{K_s^2 R_h^{4/3}}.$$

The idea is to evaluate the transport capacity $Q_{s,in}$ to be injected in the channel to maintain a fixed bottom. To do this, we simply calculate the dimensionless shear stress τ^* to be introduced in the transport capacity formula Q_s corresponding to the equilibrium (1.1). Since,

$$\tau^* = \frac{\tau}{g(\rho_s - \rho)d} = \frac{\rho R_h \partial_x z_b}{(\rho_s - \rho)d} = \frac{R_h \partial_x z_b}{Rd}, \quad (1.2)$$

where

$$R = \frac{\rho_s - \rho}{\rho},$$

by focusing on Meyer-Peter's formula & Müller and using the effective shear stress,

$$\tau_{eff} = \left(\frac{K_s}{K_p} \right)^{3/2} \tau^{star}, \quad (1.3)$$

the equilibrium transport capacity is rewritten,

$$Q_s^{MPM} = 8\sqrt{Rgd^3} \left(\left(\frac{K_s}{K_p} \right)^{3/2} \frac{R_h \partial_x z_b}{Rd} - 0.047 \right)_+^{3/2}. \quad (1.4)$$

As it stands in the Courlis code, the “quantity of sediment” injected is done through an injected concentration that can be determined as follows,

$$Q_s = \frac{C_s Q}{\rho_s} \iff C_s = \frac{\rho_s Q_s}{Q}. \quad (1.5)$$

The geometric and parametric data of the case are summarized in the table 1.1.

Channel width	$l =$	0.2	m
Channel length	$L =$	30	m
Channel slope	$I =$	0.00427	(-)
Gravity constant	$g =$	9.8	m.s^{-2}
Water density	$\rho_w =$	10^3	kg.m^{-3}
Sediment density	$\rho_s =$	2.65×10^3	kg.m^{-3}
Sediment mean diameter	$d =$	0.32×10^{-3}	m
Hydraulic discharge	$Q =$	0.0071	$\text{m}^3.\text{s}^{-1}$
water depth	$h \approx$	0.072	m
Strickler coefficient	$K_h =$	62	$\text{m}^{1/3}.\text{s}^{-1}$
	$K_s =$	62	$\text{m}^{1/3}.\text{s}^{-1}$
Grain roughness	$K_p =$	62	$\text{m}^{1/3}.\text{s}^{-1}$

Table 1.1: Parameters for the equilibrium channel test case.

The simulated time is 100 s.

1.2.2 Numerical parameters

The three mascaret kernel are tested. A time step of 0.05 s is fixed for both Sarap and Rezo kernel, and a variable time step with a Courant number fixed to 0.8 is set with mascaret.

1.3 Results

Figure 1.1 shows the initial and final profile of the bottom obtained with the Sarap kernel.

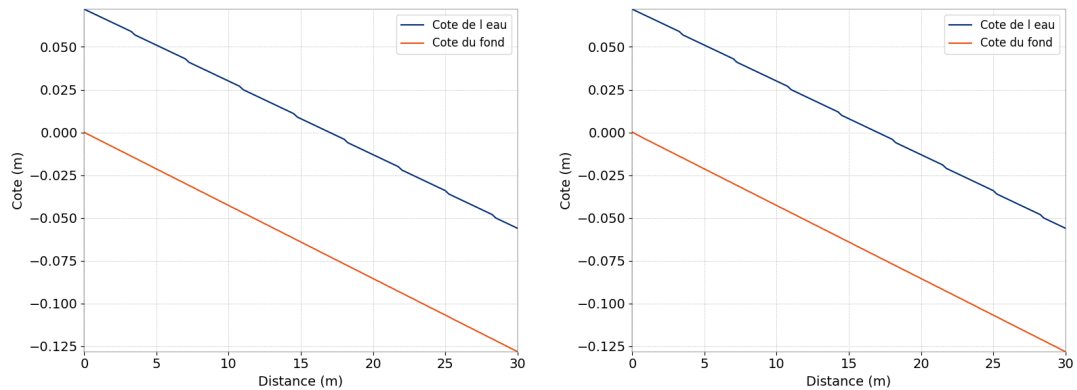


Figure 1.1: Sarap results and the initial and final time.

Figure 1.2 shows the longitudinal distribution of the bed shear stress and the solid discharge at the final time of the Sarap kernel simulation.

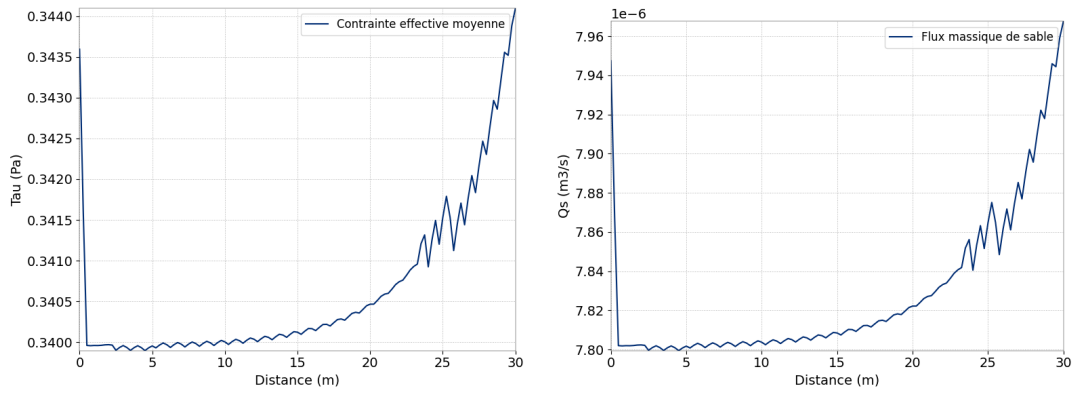


Figure 1.2: Sarap shear stress and solid discharge at the final time.

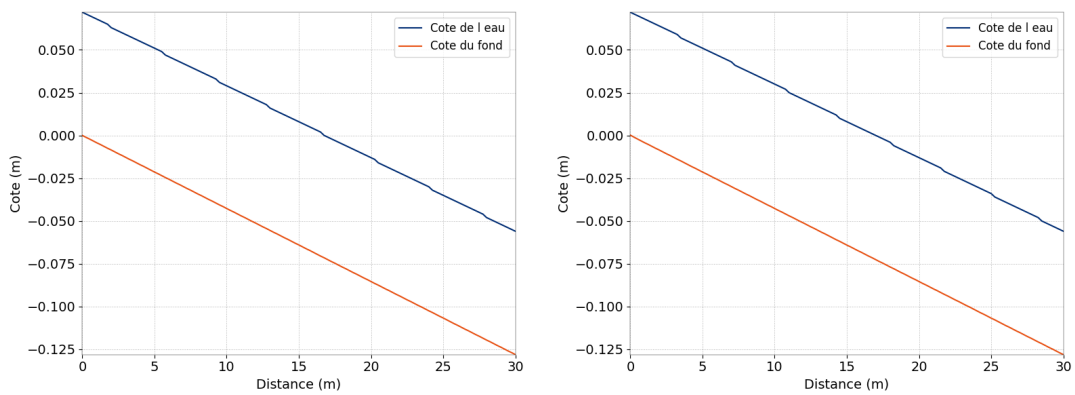


Figure 1.3: Rezo results and the initial and final time.

Figure 1.3 shows the initial and final profile of the bottom obtained with the Rezo kernel.

Figure 1.4 shows the longitudinal distribution of the bed shear stress and the solid discharge at the final time of the Rezo kernel simulation.

Figure 1.5 shows the initial and final profile of the bottom obtained with the Mascaret kernel.

Figure 1.6 shows the longitudinal distribution of the bed shear stress and the solid discharge at the final time of the Mascaret kernel simulation.

The three kernels give very similar results. Despite the non uniform longitudinal distribution of the shear stress and the associated solid discharge, the bed evolution is negligible and the initial and final profile are very similar after a 100 s simulation.

1.4 Conclusion

COURLIS is able to keep the sedimentary equilibrium on a channel.

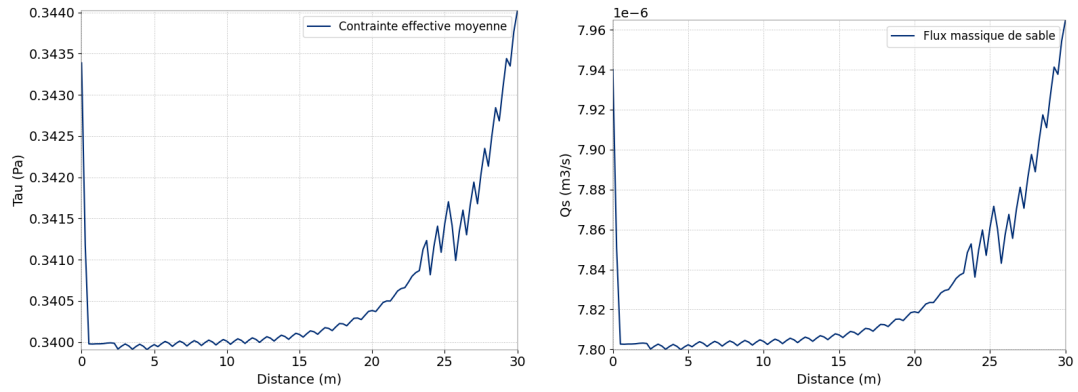


Figure 1.4: Rezo shear stress and solid discharge at the final time.

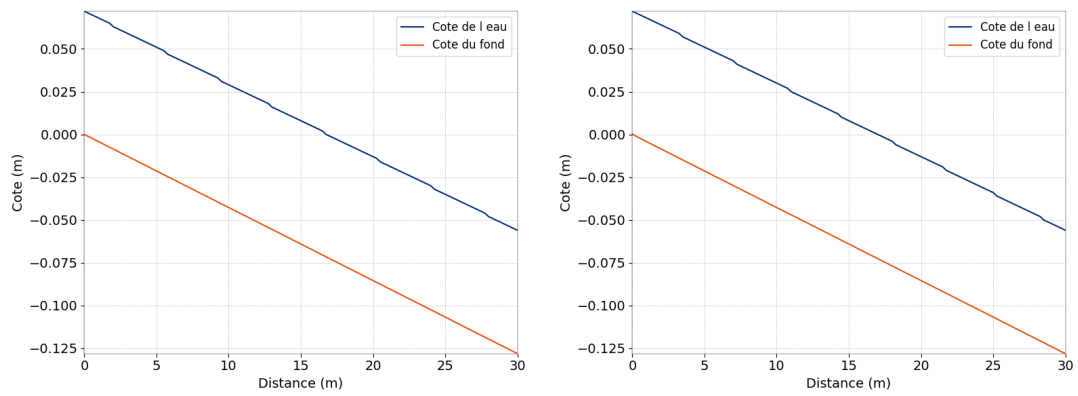


Figure 1.5: Mascaret results and the initial and final time.

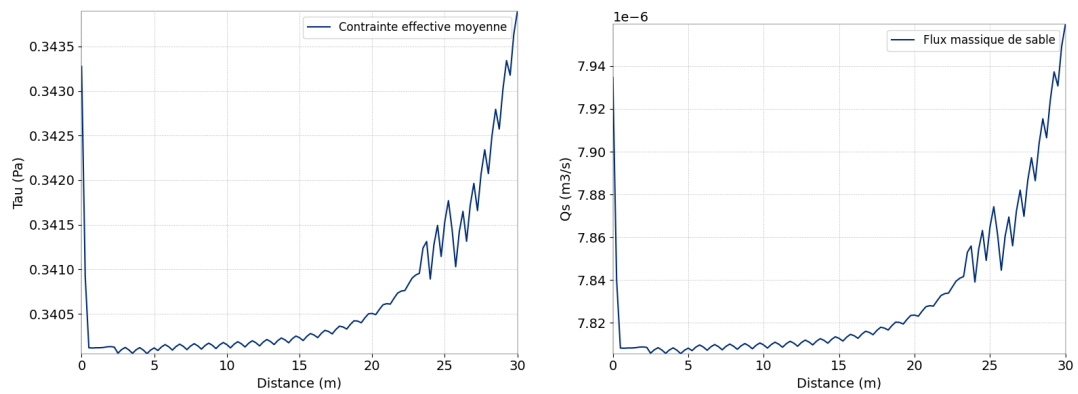


Figure 1.6: Mascaret shear stress and solid discharge at the final time.

2. Newton

2.1 Purpose

The [?]’s laboratory experiment presents the phenomenon of progressive erosion in a channel with an erodible bottom: in a rectangular channel, fed by an upstream solid flow, initially at equilibrium, the solid input is completely stopped. Measurements of the evolution of the bottom are made up to 24 hours.

2.2 Description

The experiment takes place in two steps. In a rectangular channel, a state of dynamic equilibrium is obtained with the help of a sediment supply. The channel is assumed to be in equilibrium when the amount of sediment injected upstream is completely transported downstream but also when the slope of the bottom and that of the free surface become uniform. At the downstream end, a weir was placed to maintain a constant water level during the experiment. Once equilibrium is reached, the upstream supply of sediment is stopped, which leads to a change in the bottom. The solid concentration at the inlet becomes zero and thus lower than the equilibrium concentration. To reach the latter, the system erodes the sediments of the domain and tends to find a new equilibrium state. The measurements are made during this second step, it is this part of the experiment that is modeled.

Total transport with dominant bedload was observed. This observation may give an indication of the most suitable transport formula. In addition, the presence of dunes on the bed was identified during the experiment.

Figure 2.1 shows the initial longitudinal profile of the flume.

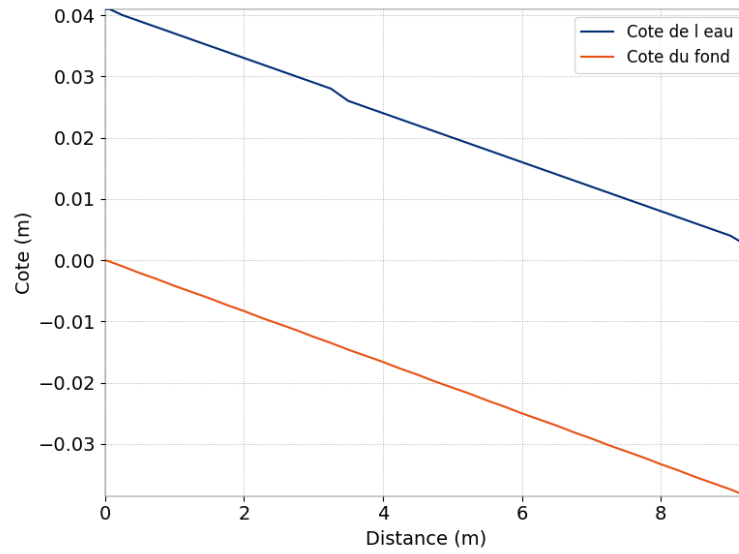


Figure 2.1: Initial longitudinal profile of the flume.

2.3 Physical parameters

Table 2.1: Geometric, hydraulic and sedimentary characteristics of Newton's experiment

Length of the channel	$L = 9.14 \text{ m}$
Width of the channel	$B = 0.3048 \text{ m}$
Slope of the channel	$I = 0.00416$
Upstream discharge	$Q = 0.00566 \text{ m}^3.\text{s}^{-1}$
Downstream water depth	$H = 0.041 \text{ m}$
Mean velocity	$V = 0.45 \text{ m.s}^{-1}$
Concentration initially injected	$C_s = 0.88 \text{ kg.m}^{-3}$
Concentration of the sand layer	$C = 1610 \text{ kg.m}^{-3}$
Median diameter of the sand	$d_{50} = 0.68 \text{ mm}$
Mass density of the sediment	$\rho_s = 2650 \text{ kg.m}^{-3}$
Settling velocity of the sand	$w_s = 0.09 \text{ m.s}^{-1}$

The Strickler coefficient is determined by a calibration on the initial water line: $K_h = 69 \text{ m}^{1/3}.\text{s}^{-1}$. The bedload transport formula chosen is Meyer-Peter and Muller formula. The friction coefficient for the transport formula has been set to $69 \text{ m}^{1/3}.\text{s}^{-1}$ and the skin friction coefficient to $88 \text{ m}^{1/3}.\text{s}^{-1}$.

2.4 Numerical parameters

The mesh size is refined at the beginning of the channel (5cm mesh). For the rest of the domain, the meshes are every 25cm.

The model is run with the 3 kernels. The time step is set to 1 s with Sarap, 0.1 s with Rezo and it is variable with mascaret, respecting a Courant number of 0.8.

2.5 Results

Figure 2.2 shows the results with the Sarap kernel in comparison with experimental data.

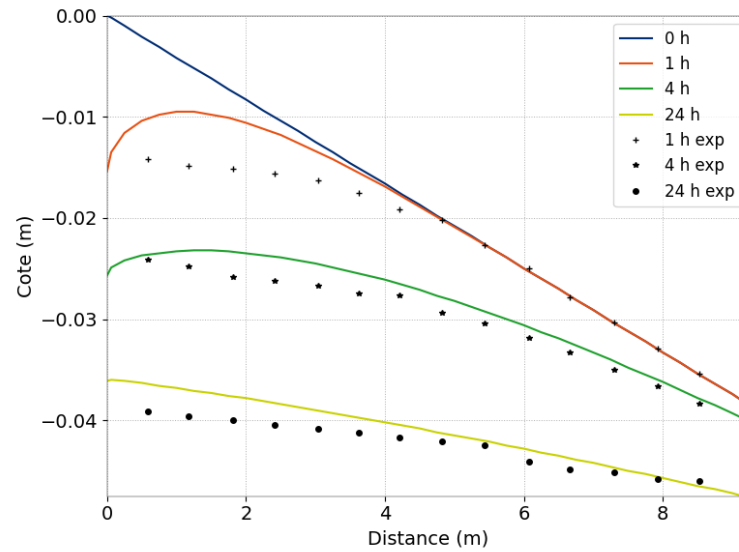


Figure 2.2: Sarap results and different times.

Figure 2.3 shows the results with the Rezo kernel in comparison with experimental data.

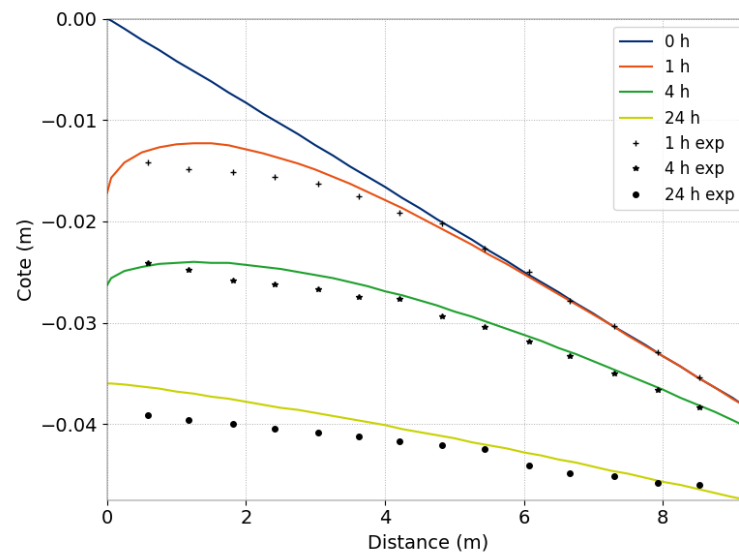


Figure 2.3: Rezo results and different times.

Figure 2.4 shows the results with the Rezo kernel in comparison with experimental data.

2.6 Conclusion

Courlis is able to represent the erosion of a laboratory channel experimental data, with every hydraulic kernels.

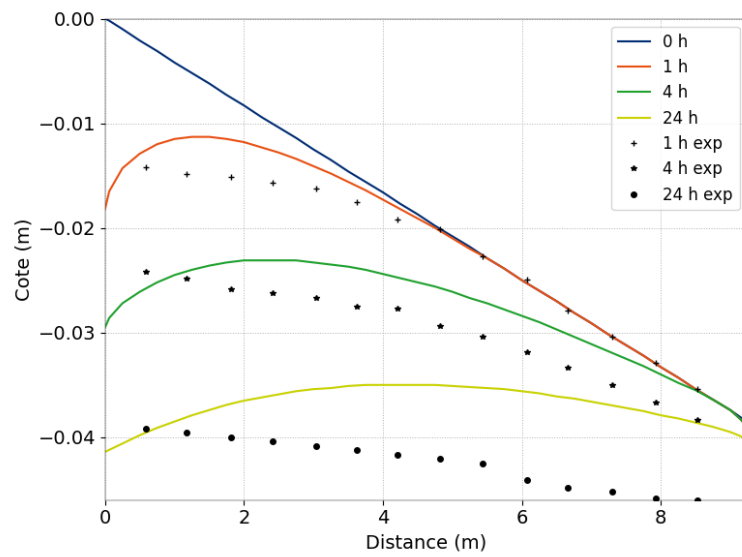


Figure 2.4: Mascaret results and diffferent times.

3. Newton trapeze

3.1 Purpose

This test case aims at validating the closure *uniform erosion – uniform deposition* imposed on the evolution of cross-section in erosion context, see the Courlis' user document. For this purpose, we have reused the same configuration as in the Newton's test case and just replaced the geometry of rectangular channel by a trapezoidal one.

3.2 Description

3.2.1 Construction of a trapezoidal channel

Given a rectangular cross-section of width L and a water height Y , we first design a simple *symetric trapezoidal* cross-section defining by 6 points P_1, \dots, P_6 as sketched in Fig. 3.1.

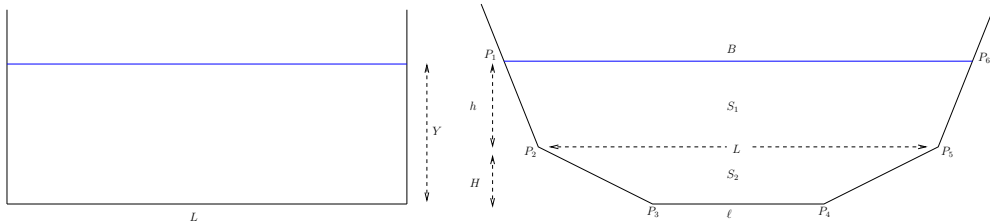


Figure 3.1: Construction a trapezoidal cross-section from a rectangular one.

Notice that we have fixed the larger base $P_2P_5 = L$ and imposed the same water height Y on the trapezoidal cross-section. In order to define the small base $P_3P_4 = \ell$, the height of the small base H and the channel width $P_1P_6 = B$ at free surface, we impose the trapezoidal cross-section to have the same wetted area and wetted perimeter than the given rectangular cross-section. It means that

$$S_1 + S_2 = YL, \quad (3.1)$$

$$2(P_1P_2 + P_2P_3) + \ell = 2Y + L. \quad (3.2)$$

where S_1, S_2 are the areas of the upper et lower trapezoid as sketched in Fig. 3.1.

Introducing the following dimensionless parameters

$$\alpha = \frac{H}{Y}, \quad \beta = \frac{\ell}{L} \quad (0 < \alpha, \beta < 1),$$

and for a given value of α , the condition (3.1) leads to

$$\frac{B}{L} = 1 + \frac{\alpha(1-\beta)}{1-\alpha}$$

where β can be computed from condition (3.2). Indeed, by defining

$$\varepsilon = \frac{Y}{L}$$

which is determined from the rectangular channel, and using the parameter change

$$2\varepsilon x = 1 - \beta,$$

x is solution of equation

$$\sqrt{\alpha^2 + x^2} + \sqrt{(1-\alpha)^2 + \left(\frac{\alpha}{1-\alpha}\right)^2 x^2} = 1 + x. \quad (3.3)$$

This later equation can be solved numerically. For the Newton test case ($L = 0.3048$, $Y = 0.041$, $\varepsilon = 0.134$), the solution x of (3.3), and the ratios $\ell/L, B/L$ in function of α are plotted in Fig. 3.2.

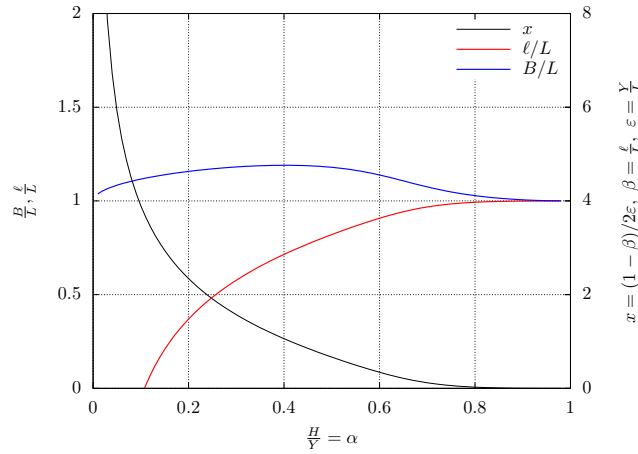


Figure 3.2: Solution of equation (3.3) for the Newton test case.

3.2.2 Parameters

Now, applying these equations for the Newton test case and by fixing $\alpha = 0.2$, one can find $\beta = 0.3697$ and $B/L = 1.1576$. The resulting trapezoidal cross-section is sketched in the left plot of Fig. 3.3.

Next, for the chosen closure *uniform erosion – uniform deposition*, we have imposed the width of erosion parameter being the larger base $P_2P_3 = L$. Recall that according to this closure, the trapezoid $P_2P_3P_4P_5$ will be displaced downward with some distance δz in case of erosion as sketched in the right plot of Fig. 3.3.

3.3 Results

Figure 3.4 shows the results with the Sarap kernel. Figure 3.5 shows the results with the Rezo kernel. One can note that the feature has not yet been implemented in the mascaret kernel. In particular, the number of call on the planimetry routine is shown in the left plots. One can find that re-planimetry was only carried out where the river bottom is eroded.

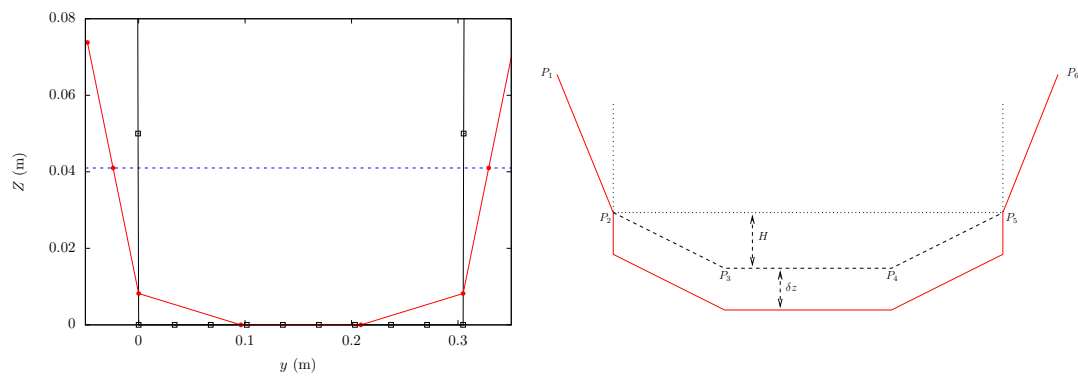


Figure 3.3: Left: initial cross-section. Right: expected cross-section for erosion case (dotted line is the corresponding rectangular profile).

3.4 Conclusion

The evolution of cross-sections is correctly reproduced.

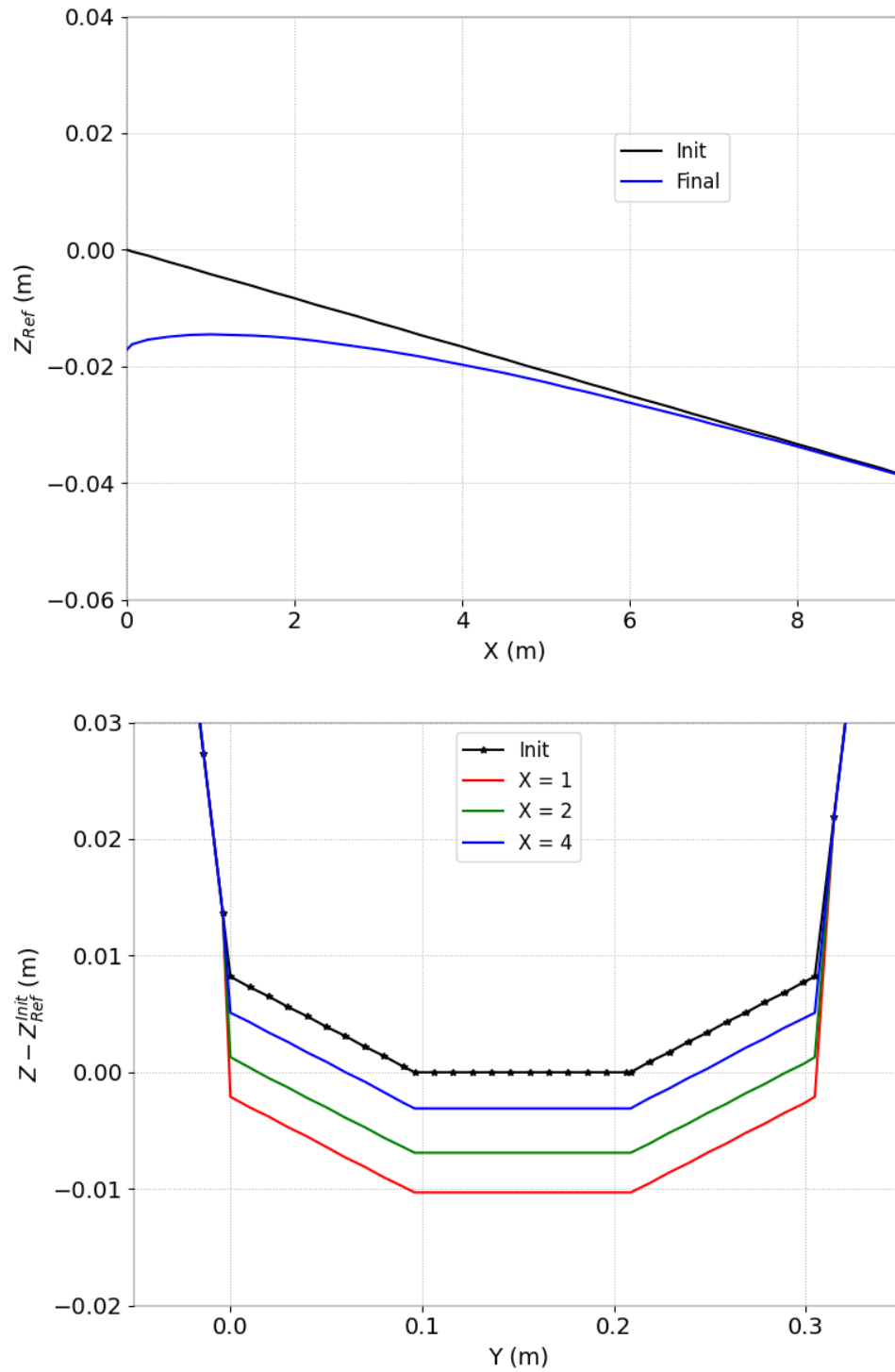


Figure 3.4: Longitudinal and transversal profiles given by the Sarap kernel.

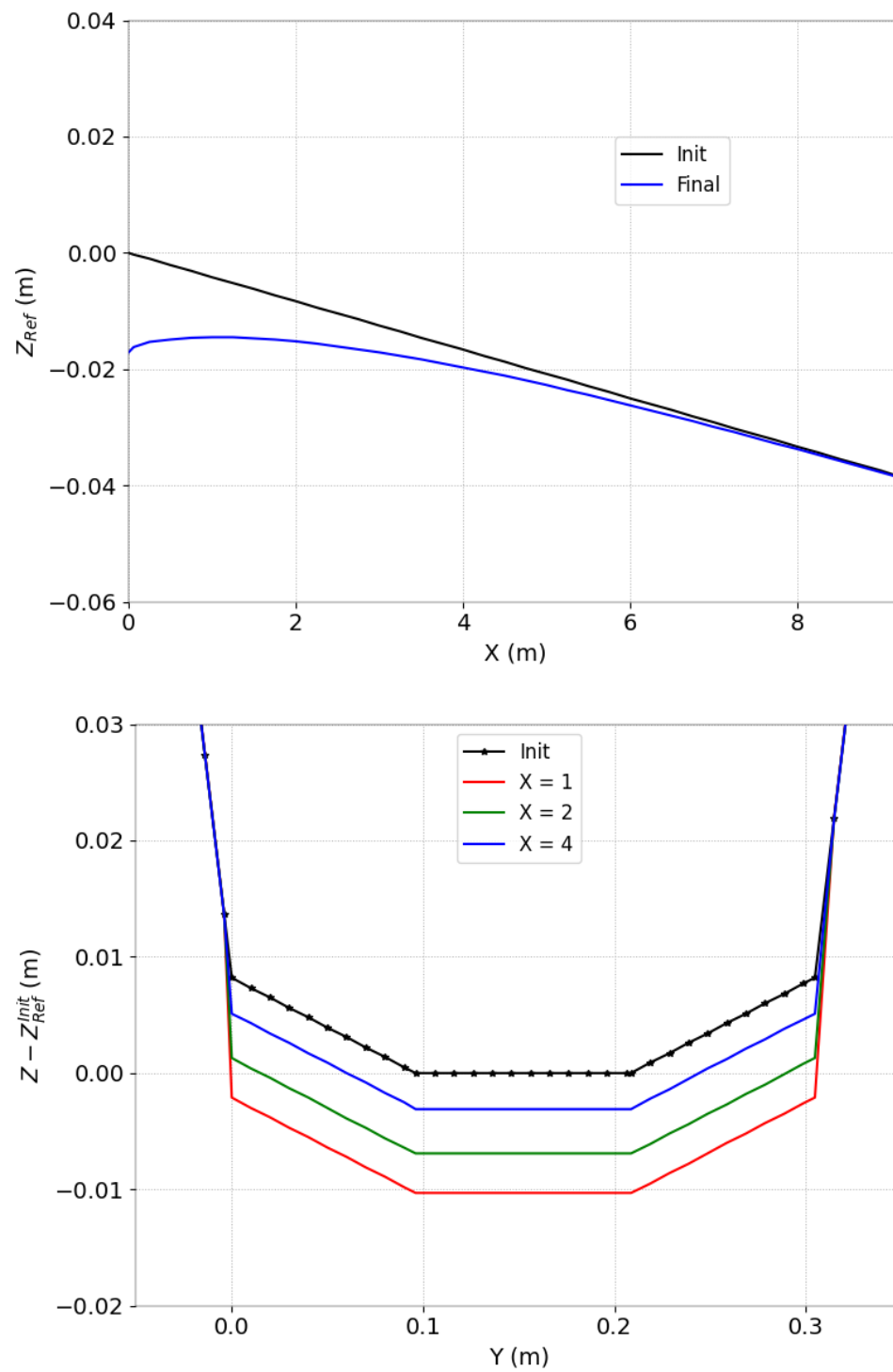


Figure 3.5: Longitudinal and transversal profiles given by the Rezo kernel.

4. Soni

4.1 Purpose

The laboratory experiment of [3] reports the phenomenon of deposition following a sudden increase in the supply of sediments in a channel.

4.2 Description

The experiment is carried out in a rectangular channel covered with an erodible bed of uniform sandy sediment. It is carried out in two stages. The first one consists in reaching a dynamic equilibrium state under a fixed constant flow. After having obtained a stable equilibrium slope, an addition of sediments superior to the transport capacity is injected at the entrance of the channel. This addition results in a deposit in the system and the measurements of the evolution of the funds begin. It is this second step that is modeled.

During the experiment, the presence of ripples and dunes was observed and more particularly in the part where the deposit is not pronounced. The measurements presented are averaged.

Figure 4.1 shows the initial longitudinal profile of the flume.

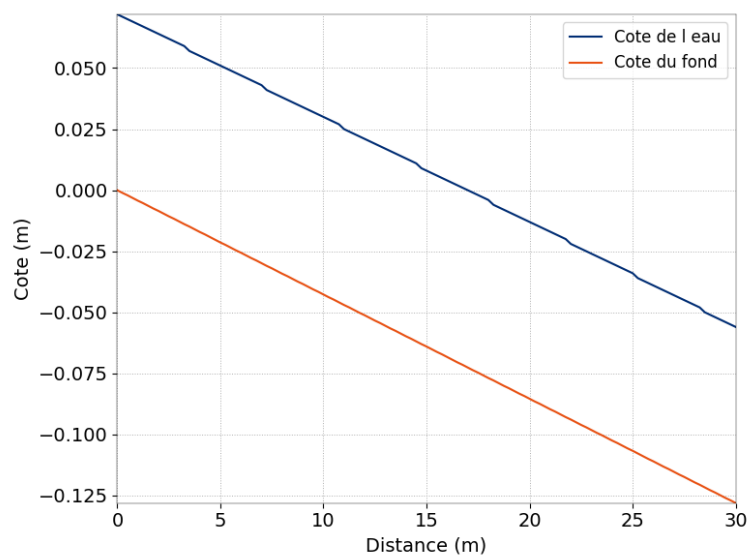


Figure 4.1: Initial longitudinal profile of the flume.

4.3 Physical parameters

Table 4.1: Geometric, hydraulic and sedimentary characteristics of Newton's experiment

Length of the channel	$L = 30 \text{ m}$
Width of the channel	$B = 0.2 \text{ m}$
Slope of the channel	$I = 0.00427$
Upstream discharge	$Q = 0.00571 \text{ m}^3.\text{s}^{-1}$
Downstream water depth	$H = 0.072 \text{ m}$
Mean velocity	$V = 0.49 \text{ m.s}^{-1}$
Concentration initially injected	$C_s = 4.88 \text{ kg.m}^{-3}$
Concentration of the sand layer	$C = 1650 \text{ kg.m}^{-3}$
Median diameter of the sand	$d_{50} = 0.32 \text{ mm}$
Mass density of the sediment	$\rho_s = 2650 \text{ kg.m}^{-3}$
Settling velocity of the sand	$w_s = 0.042 \text{ m.s}^{-1}$

The Strickler coefficient is determined by a calibration on the initial water line: $K_h = 62 \text{ m}^{1/3}.\text{s}^{-1}$. The bedload transport formula chosen is Meyer-Peter and Muller formula. The friction coefficient for the transport formula has been set to $62 \text{ m}^{1/3}.\text{s}^{-1}$ and the skin friction coefficient to $62 \text{ m}^{1/3}.\text{s}^{-1}$.

4.4 Numerical parameters

The mesh size is refined at the beginning of the channel (5cm mesh). For the rest of the domain, the meshes are every 25cm.

The model is run with the 3 kernels. The time step is set to 0.5 s with Sarap, 0.15 s with Rezo and it is variable with mascaret, respecting a Courant number of 0.8.

4.5 Results

Figure 4.2 shows the results with the Sarap kernel in comparison with experimental data.

Figure 4.3 shows the results with the Rezo kernel in comparison with experimental data.

Figure 4.4 shows the results with the Rezo kernel in comparison with experimental data.

4.6 Conclusion

Courlis is able to represent the deposition process of a laboratory channel experimental data, with every hydraulic kernels.

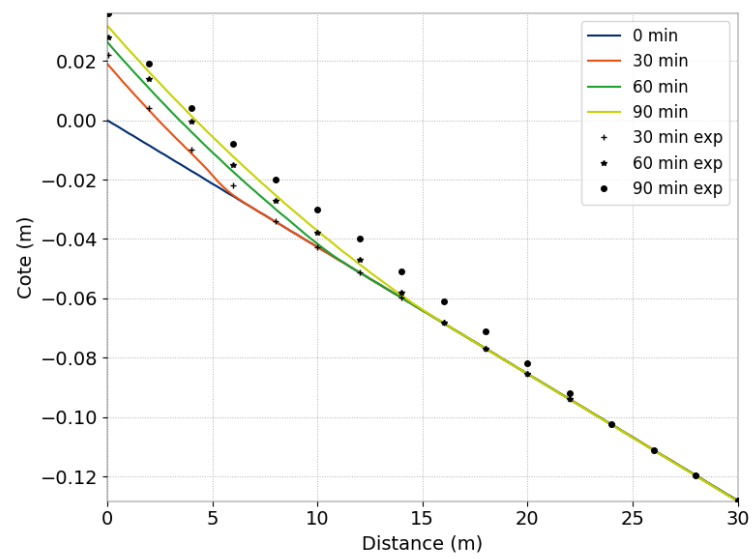


Figure 4.2: Sarap results and different times.

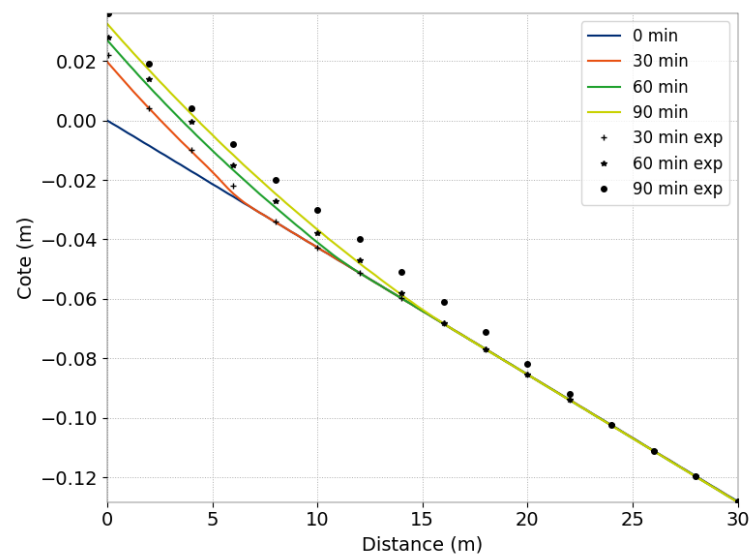


Figure 4.3: Rezo results and different times.

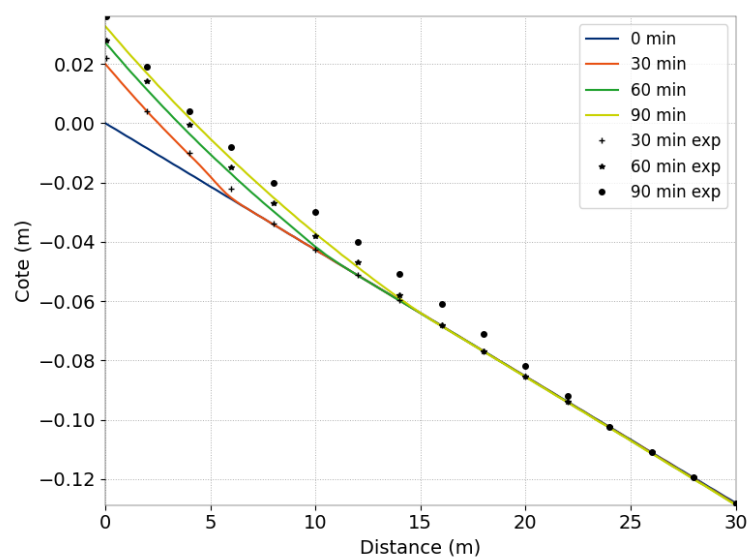


Figure 4.4: Mascaret results and diffferent times.

5. Soni trapeze

5.1 Purpose

This test case aims at validating the closure *uniform erosion – uniform deposition* imposed on the evolution of cross-section in deposition context, see the Courlis' user document. For this purpose, we have reused the same configuration than the Soni test case and just replaced the geometry of rectangular channel by a trapezoidal one.

5.2 Description

We refer to Chapt. 3 for the equations on construction of a trapezoidal cross-section from a given rectangular one. Now, applying these equations for the Soni test case for which $\varepsilon = 0.35$ and by fixing $\alpha = 0.4$, one can find $\beta = 0.2368$ and $B/L = 1.5088$. The resulting trapezoidal cross-section is sketched in Fig. 5.1.

Next, for the chosen closure *uniform erosion – uniform deposition*, we have imposed the width of erosion parameter being the larger base $P_2P_3 = L$. Recall that according to this closure, the trapezoid $P_2P_3P_4P_5$ will be moved upward with some distance δz in case of deposition.

5.3 Results

Figure 5.2 shows the results with the Sarap kernel. Figure 5.3 shows the results with the Rezo kernel. One can note that the feature is not yet available with the Mascaret kernel. In particular, the number of call on the planimetre routine is shown in the left plots. One can find that re-planimetre was only carried out where the river bottom is deposited.

5.4 Conclusion

The evolution of cross-sections is correctly reproduced.

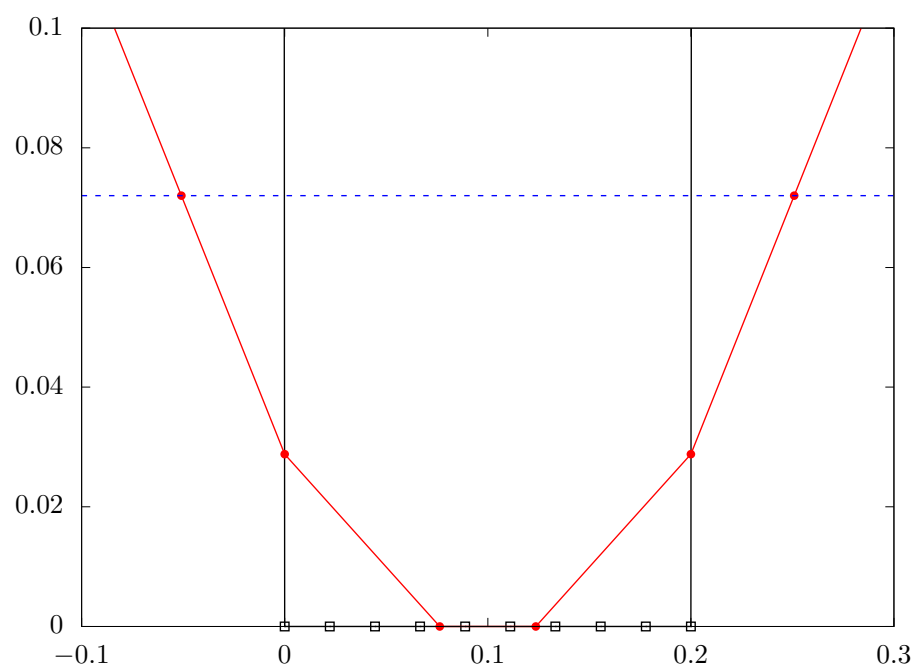


Figure 5.1: Initial cross-section.

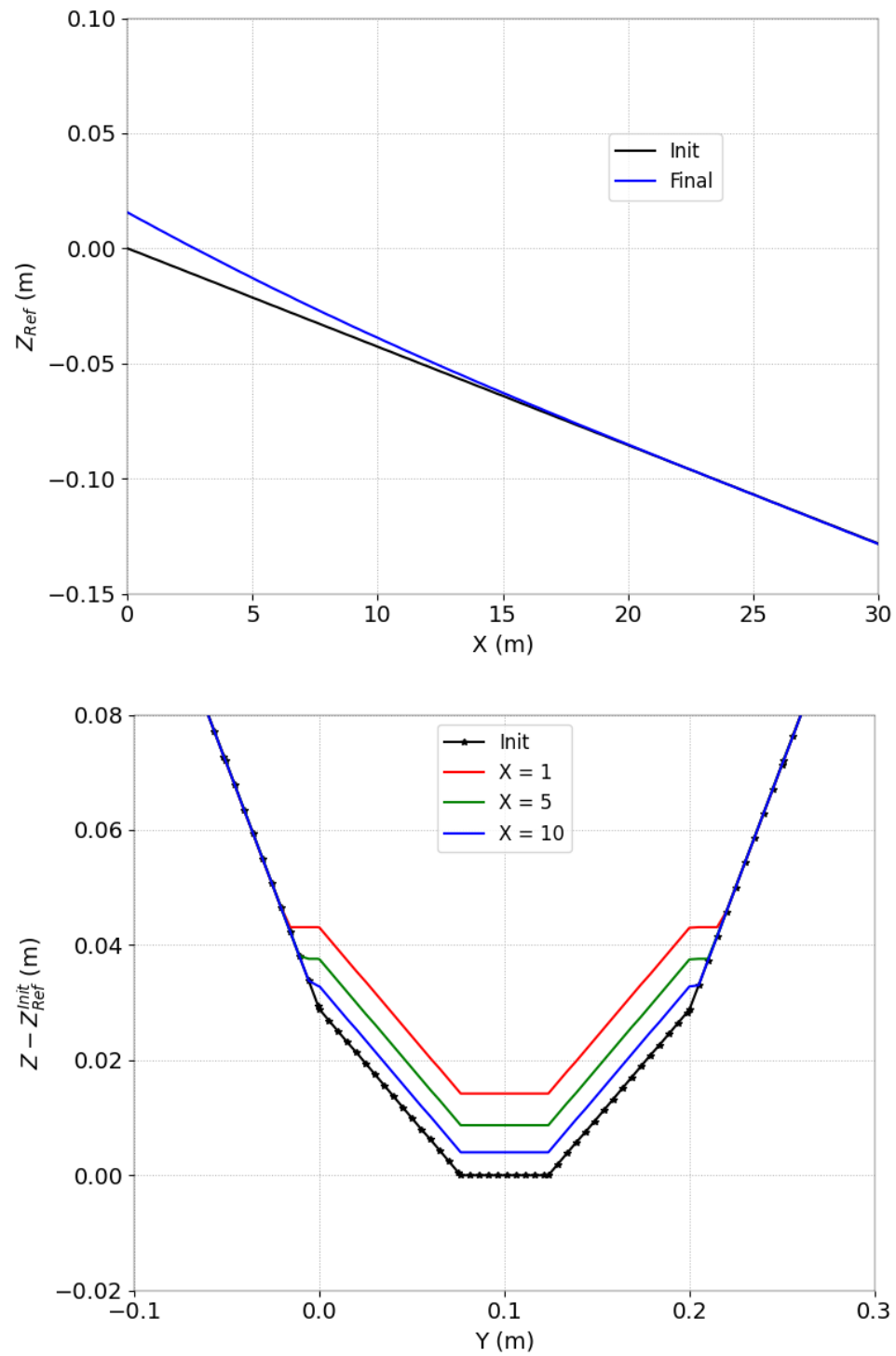


Figure 5.2: Longitudinal and transversal profiles given by the Sarap kenel.

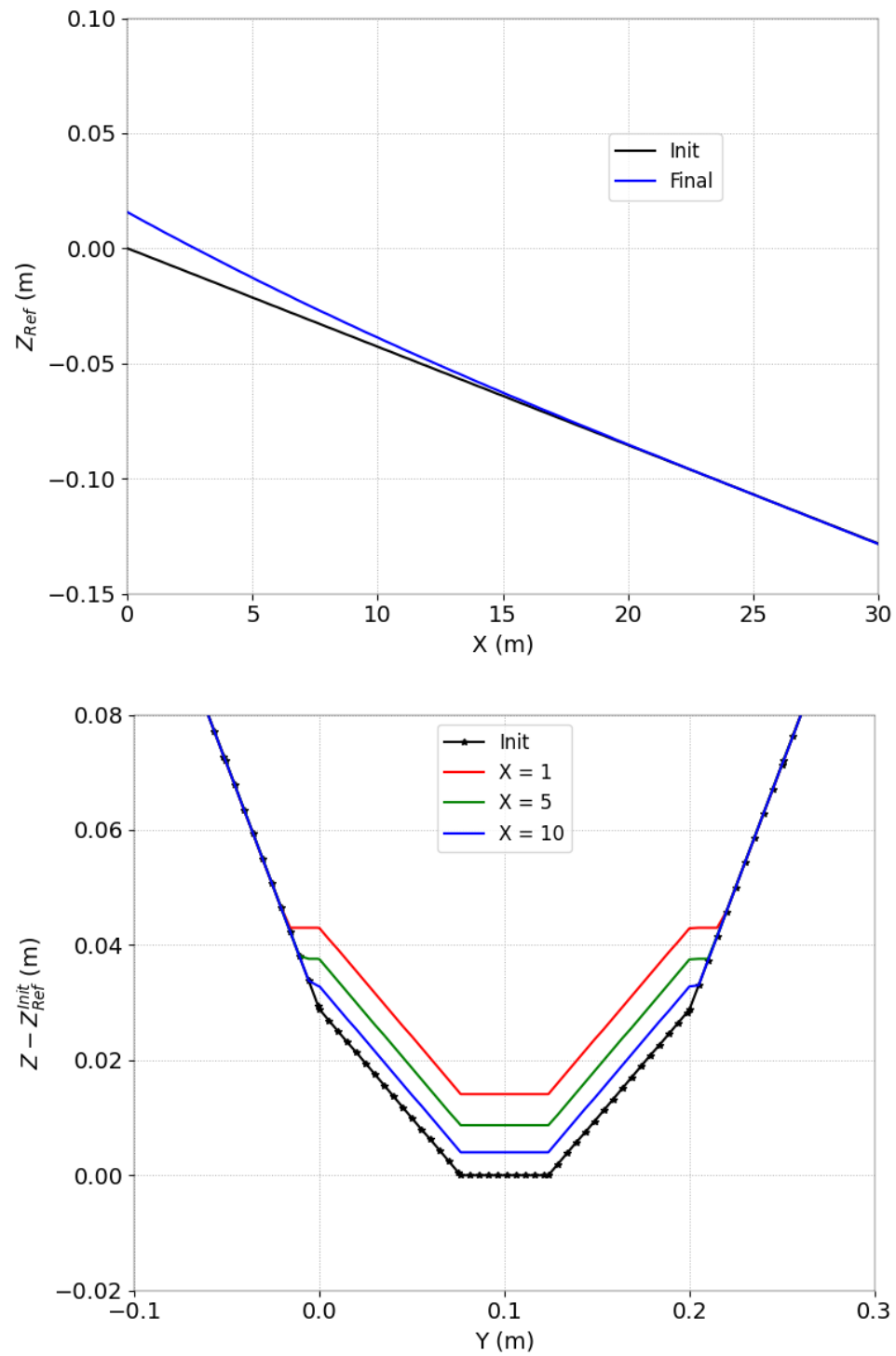


Figure 5.3: Longitudinal and transversal profiles given by the Rezo kernel.

6. Van Rijn

6.1 Purpose

This test case tests the non-cohesive sediment transport in suspension.

6.2 Description

This experiment, conducted by Van Rijn at the Delft Hydraulics Laboratory, consists in studying the phenomenon of progressive erosion associated with the trapping of sediments in a pit in the presence of a stationary and uniform flow with a dominant mode of transport which is suspension. The local excavations are too short for the water level to drop at the deepened part, it remains imposed by the downstream reach, preventing acceleration upstream. In the area of the excavation, the water level increases and the flow velocity decreases. The transport capacity of the flow decreases, the sediments coming from upstream are trapped in the pit. Downstream, the head decreases and the velocity increases, the transport capacity increases and the flow must therefore take material to restore the solid flow to its initial level (Figure 1). Thus, progressive deposition in the pit and progressive erosion in the downstream portion of the channel are expected. Overall, the pit moves downstream and deforms.

6.3 Physical parameters

The physical parameters of the model are:

Figure 6.1 shows the initial water depth and bottom elevation.

6.4 Numerical parameters

The longitudinal space step is 50 m. The mascaret kernel is used with a variable time step and a Courant number of 0.8.

6.5 Results

Figure 6.2 shows the computed water depth and bottom elevation with a comparison with experimental data.

6.6 Conclusion

COURLIS is able to model the non-cohesive suspended sediment of the Van Rijn experiment.

Table 6.1: Geometric, hydraulic and sedimentary characteristics

Channel length	$L = 30$ m
Channel width	$B = 0.5$ m
Channel slope	$I = 0.001517$
Pit length	$L_f = 3$ m
Pit slope	$p_f = 0.1$
Pit depth	$h_f = 0.15$ m
Upstream inflow	$Q = 0.09945$ m ³ .s ⁻¹
Downstream water depth	$H = 0.39$ m
Strickler coefficient	$K = 43$ m ^{1/3} .s ⁻¹
Initial concentration	$C_s = 0.21$ kg.m ⁻³
Soil sand concentration	$C = 1590$ kg.m ⁻³
Mean diameter	$d_{50} = 0.16$ mm
Settling velocity	$w_s = 0.013$ m.s ⁻¹

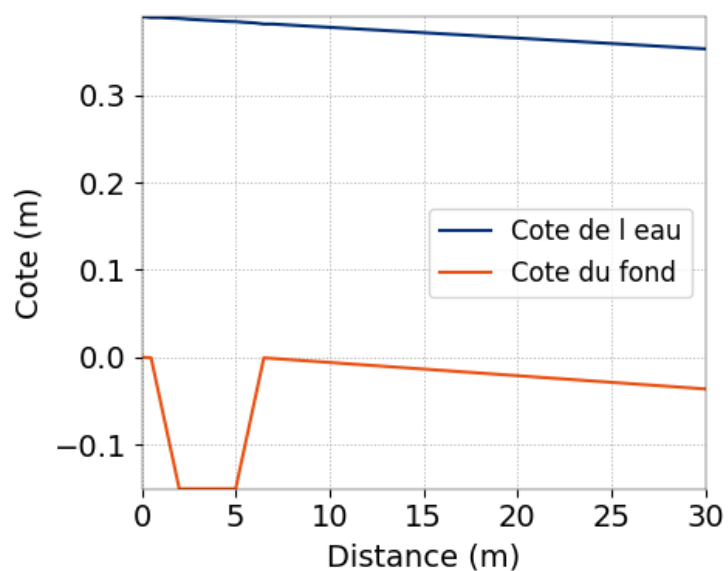


Figure 6.1: Initial configuration.

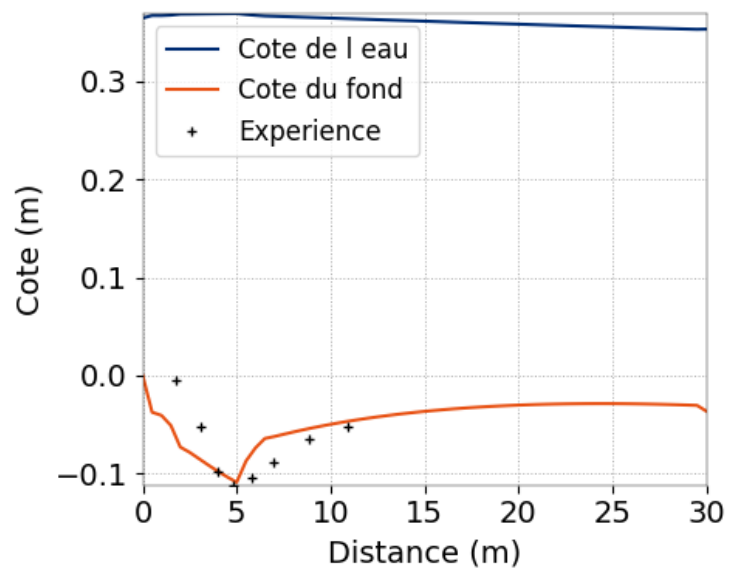


Figure 6.2: Final results.

7. Bedload formulae test

7.1 Purpose

This test case tests the 4 bedload transport formulae in 6 tests each.

7.2 Description

7.2.1 Physical parameters

For each bedload formula a case number is associated (Meyer-Peter and Muller [1]: 0, Lefort: 1, Recking 2013 [2]: 2, Recking 2015: 3).

The base configuration is an inflow slope of 1% with an imposed upstream discharge of 100 m³/s. Its sediment distribution, noted D₁ is d₈₄=0.0573 m, d_m=0.03 m, d₁₆=0.00573 m, d₅₀=0.27285714 m. The influence of the slope is studied with cases with 2% slope and 0.5% slope. Then the inflow vary from 20 m³/s to 300 m³/s. A second distribution (D₂) of the sediment size is also tested: d₈₄=0.09545455 m, d_m=0.05 m, d₁₆=0.00954545 m, d₅₀=0.4545455 m.

Table 7.1 summarize all the tested configuration:

7.2.2 Numerical parameters

The mascaret kernel used is Sarap, with a duration of 2 s and a time step of 1 s.

7.3 Results

Figure 7.1 compares the numerical solution given by the code to a reference solution for each test case. It shows a very good agreement between simulated and expected results.

7.4 Conclusion

Courlis is able to reproduce the accurate bedload fluxes for different transport formulae, slope conditions, input discharges and grain size distribution.

Table 7.1: Configurations tested.

Case number	Formula	Slope (%)	Inflow (m ³ /s)	Sediment distribution
000	Meyer-Peter and Muller	1	100	D ₁
011	Meyer-Peter and Muller	0.5	100	D ₁
012	Meyer-Peter and Muller	2	100	D ₁
021	Meyer-Peter and Muller	1	300	D ₁
022	Meyer-Peter and Muller	1	20	D ₁
031	Meyer-Peter and Muller	1	100	D ₂
100	Lefort	1	100	D ₁
111	Lefort	0.5	100	D ₁
112	Lefort	2	100	D ₁
121	Lefort	1	300	D ₁
122	Lefort	1	20	D ₁
131	Lefort	1	100	D ₂
200	Recking 2013	1	100	D ₁
211	Recking 2013	0.5	100	D ₁
212	Recking 2013	2	100	D ₁
221	Recking 2013	1	300	D ₁
222	Recking 2013	1	20	D ₁
231	Recking 2013	1	100	D ₂
300	Recking 2015	1	100	D ₁
311	Recking 2015	0.5	100	D ₁
312	Recking 2015	2	100	D ₁
321	Recking 2015	1	300	D ₁
322	Recking 2015	1	20	D ₁
331	Recking 2015	1	100	D ₂

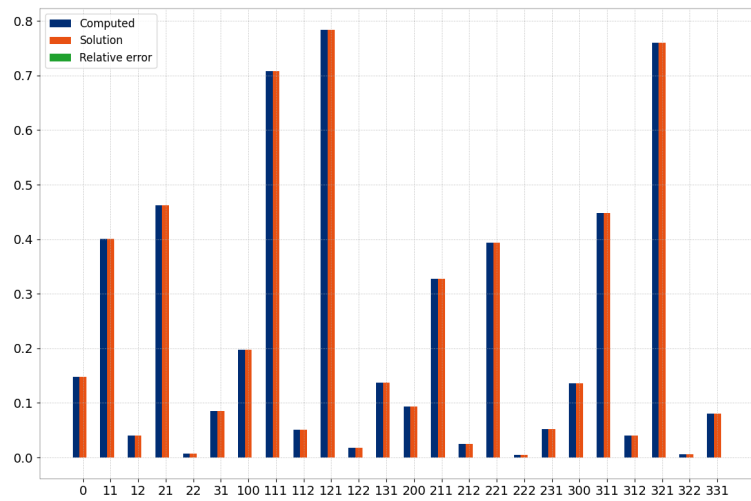


Figure 7.1: Comparison between simulated and expected bedload fluxes.

8. Cohesive channel

8.1 Erosion

8.1.1 Purpose

The purpose of this test case is to validate the calculation of the erosion flux and the evolution of the suspended sediment concentration along the reach.

8.1.2 Description

To obtain an analytical solution, the bathymetry evolution is not updated due to erosion (fixed bottom). The hydraulic kernel REZO is used. We are interested in the erosion of the bottom in a rectangular channel. Friction is considered to be zero on the bottom and on the walls.

8.1.3 Physical parameters

The river is a rectangular channel with flat bottom, length L , width La , zero slope.

Table 8.1: Parameters of test case: erosion in a rectangular channel

L	1500	m	Length of the channel
La	50	m	Width of the channel
M	10^{-2}	$\text{kg m}^{-2} \text{s}^{-1}$	Partheniades constant
τ_{ce}	0.01	Pa	Critical erosion stress
C_0	0	g/l	Concentration entering the channel
Q	50	$\text{m}^3 \text{s}^{-1}$	Flow rate into the channel
H	4.5	m	Head of water downstream
K_p	85	$\text{m}^{1/3} \text{s}^{-1}$	Skin Strickler coefficient

We consider the flow initially as uniform and permanent with an initial concentration of zero sediment.

Being in river flow, we impose two boundary conditions:

- upstream, a constant flow Q and concentration C_0 ;
- downstream, a constant elevation and a free sediment flow.

To highlight erosion, additional assumptions must be made: Deposition must be zero, therefore the settling velocity of the mud will be zero.

8.1.4 Analytical solution

The equation to solve is:

$$U \frac{\partial C}{\partial x} - k_x \frac{\partial^2 C}{\partial x^2} = \frac{\Phi_{erosion}}{A}, \quad (8.1)$$

with as boundary conditions $C(x=0) = C_0$ and $\left(\frac{\partial C}{\partial x}\right)_{x=L} = 0$, with H , the water depth, and the erosion flux according to Partheniades law, the equation (8.1) becomes:

$$U \frac{\partial C}{\partial x} - k_x \frac{\partial^2 C}{\partial x^2} = \frac{M(\tau/\tau_{ce} - 1)}{H}. \quad (8.2)$$

In the case where the diffusion is zero, $k_x = 0$, and the equation (8.2) turns into a simple first-order differential equation, whose solution is:

$$C(x) = \alpha \frac{x}{L} + C_0, \quad (8.3)$$

where $\alpha = \frac{LM(\tau/\tau_{ce}-1)}{UH}$, where $\tau = \rho g H(x,y) J = \frac{\rho g H(x,y) u^2}{K_p^2 R_h^{4/3}}$

If the scattering is not zero, $k_x \neq 0$, the equation (8.2) is rewritten in terms of the Peclet number, $Pe = \frac{UL}{k_x}$, and α . The Peclet number represents the ratio of convection to diffusion. The equation is then written:

$$\frac{1}{Pe} \frac{\partial^2 C}{\partial x^2} - \frac{1}{L} \frac{\partial C}{\partial x} = -\frac{\alpha}{L^2}, \quad (8.4)$$

whose solution can be written:

$$C(x) = C_0 + \alpha \frac{x}{L} + \frac{\alpha}{Pe} \left(e^{-Pe} - e^{-Pe(1-x/L)} \right). \quad (8.5)$$

We study the results of this test case for two different values of Peclet number : an infinite Peclet number (there is no diffusion) and a Peclet number of 1 (the diffusion is as important as the convection). The corresponding diffusion coefficients are 0 and 333.3 m²/s.

For a Peclet equal to 1, diffusion has the effect of decreasing the concentration of SS from the first meters of the reach, and consequently the concentration at the end of the channel is three times lower than the case without diffusion.

8.1.5 Numerical parameters

The duration is set to 136 000 s and the time step is 108 s. The discretization of the reach is 30 m.

8.1.6 Results

Figure 8.1 and 8.2 show the suspended sediment concentration along the channel simulated, in comparison with the analytical solution.

8.1.7 Conclusion

The erosion flux is well represented.

8.2 Deposition

8.2.1 Purpose

The purpose of this test case is to validate the calculation of the deposition flux and the evolution of the suspended sediment load concentration along the reach.

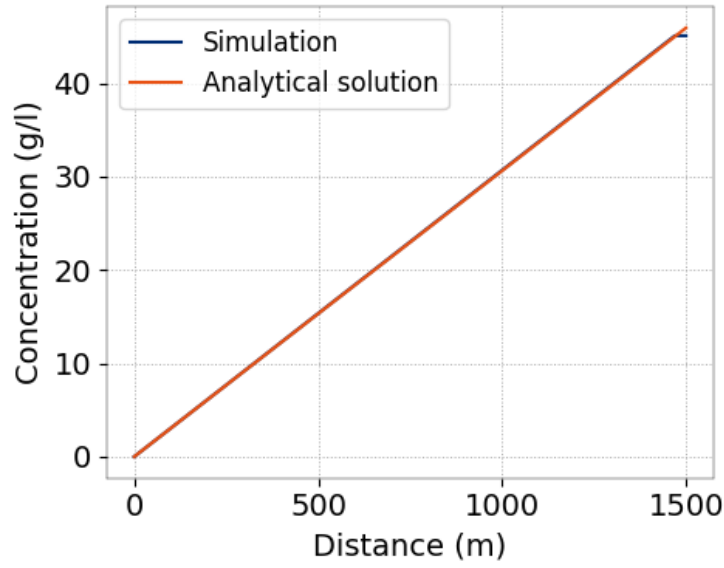


Figure 8.1: Concentration along the channel without diffusion, simulation vs analytical solution.

8.2.2 Description

In order to obtain an analytical solution, the bathymetry evolution is not updated after the deposition (fixed bottom). We place ourselves here in the case of a river flow. The hydraulic calculation kernel REZO is therefore used. We are interested in a deposition phenomenon with entry of SS in the reach. Friction is considered to be nil on the bottom and on the walls.

8.2.3 Physical parameters

One considers a rectangular channel with flat bottom, of length L , width La , and zero slope.

L	1500	m	Length of the channel
La	50	m	Width of the channel
ws	$1.5 \cdot 10^{-4}$	m/s	Settling velocity of the mud
τ_{cd}	0.1	Pa	Critical deposition shear stress
$C0$	1	g/l	Inflow concentration
Q	10	$\text{m}^3 \text{s}^{-1}$	Channel discharge
H	4.5	m	Water depth
Kp	85	$\text{m}^{1/3} \text{s}^{-1}$	Skin friction coefficient

Table 8.2: Parameters of deposition test case.

Being in fluvial flow, one imposes two boundary conditions:

- upstream, a constant flow and concentration Q and $C0$;
- downstream, a constant elevation and a free sediment flow.

Since we will be highlighting deposition, additional assumptions must be made:

- the erosion must be null, that is why the coefficient of Parthéniades will be taken null;

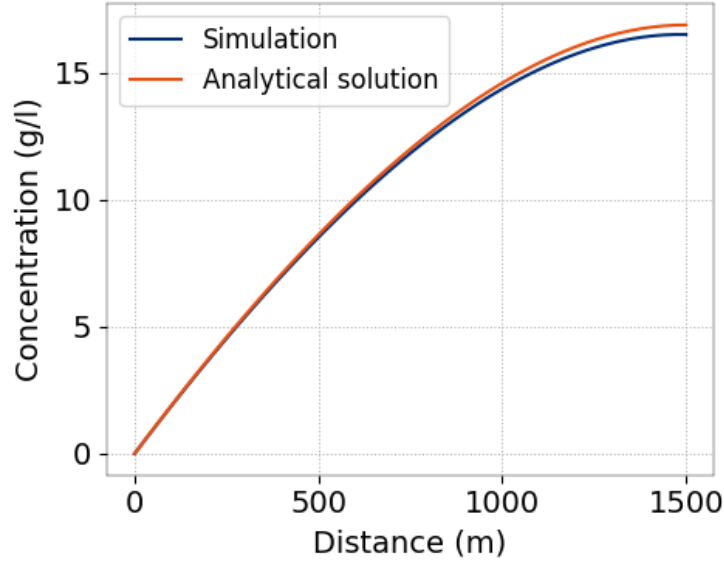


Figure 8.2: Concentration along the channel with diffusion, simulation vs analytical solution.

- we study an established regime, to obtain the update of the geometry of the bottom of the channel following the deposit is not carried out.

8.2.4 Analytical solution

Under these assumptions and this geometry, the equation to be treated becomes:

$$U \frac{\partial C}{\partial x} - k_x \frac{\partial^2 C}{\partial x^2} = \frac{\Phi_{depot}}{A} \quad (8.6)$$

with the boundary conditions defined as $C(x=0) = C_0$ and $\left(\frac{\partial C}{\partial x}\right)_{x=L} = 0$, with H the water depth, and the deposition flux given by the Krone law, equation (8.6) becomes :

$$U \frac{\partial C}{\partial x} - k_x \frac{\partial^2 C}{\partial x^2} = \frac{C w_s (1 - \tau / \tau_{cd})}{H} \quad (8.7)$$

Under the assumptions of non-variation of the geometry, this differential equation has an analytical solution because these coefficients are constant.

In the case of zero diffusion, $k_x = 0$, the equation (8.6) turns into a simple first order differential equation:

$$\frac{\partial C}{\partial x} = -\frac{\alpha}{L} C, \quad (8.8)$$

where $\alpha = \frac{L w_s (1 - \tau / \tau_{cd})}{U H}$.

dont la solution est :

$$C(x) = C_0 e^{-\alpha x / L}. \quad (8.9)$$

If $k_x \neq 0$, the equation (8.6) is written depending on the Peclet number, $Pe = \frac{UL}{k_x}$, and on α :

$$\frac{1}{Pe} \frac{\partial^2 C}{\partial x^2} - \frac{1}{L} \frac{\partial C}{\partial x} = -\frac{\alpha}{L^2}, \quad (8.10)$$

then the solution writes:

$$C(x) = \frac{\omega_2 e^{\omega_2} e^{\omega_1 x/L} - \omega_1 e^{\omega_1} e^{\omega_2 x/L}}{\omega_2 e^{\omega_2} - \omega_1 e^{\omega_1}}, \quad (8.11)$$

with

$$\omega_1 = \frac{1 + \sqrt{1 + 4\alpha/Pe}}{2/Pe}, \quad (8.12)$$

$$\omega_2 = \frac{1 - \sqrt{1 + 4\alpha/Pe}}{2/Pe}. \quad (8.13)$$

As for erosion, the phenomenon of diffusion is introduced with a Peclet number of 1 (with a value of diffusion coefficient equal to 75 m²/s), an infinite Peclet number is also tested ($k_x = 0$ m²/s).

8.2.5 Numerical parameters

The duration is set to 300 000 s and the time step is 80 s. The discretization of the reach is 30 m.

8.2.6 Results

Figure 8.3 and 8.4 show the suspended sediment concentration along the channel simulated, in comparison with the analytical solution.

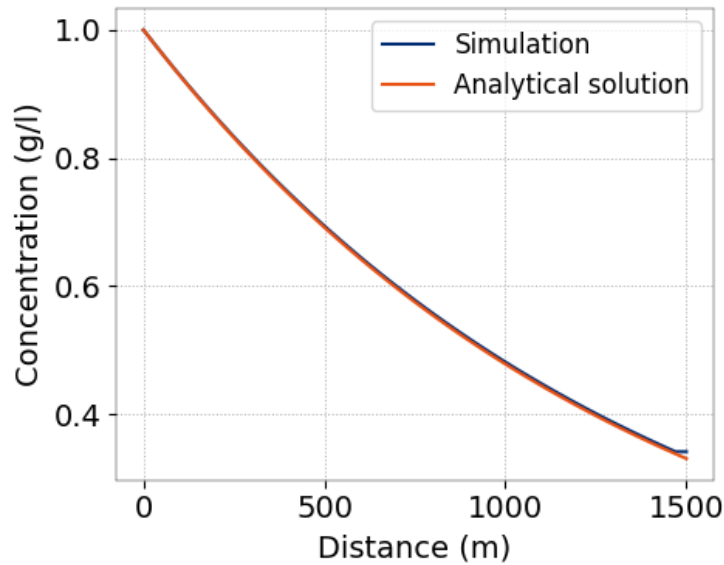


Figure 8.3: Concentration along the channel without diffusion, simulation vs analytical solution.

8.2.7 Conclusion

The deposition flux is well represented.

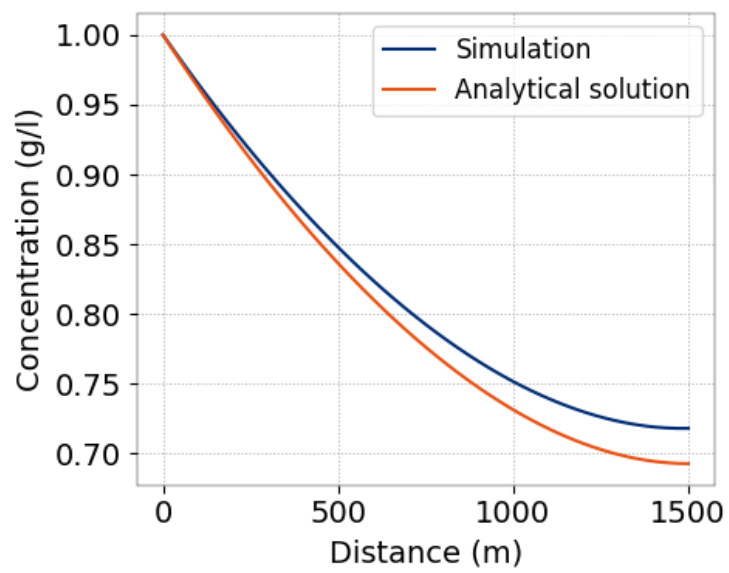


Figure 8.4: Concentration along the channel with diffusion, simulation vs analytical solution.

9. Dambreak

9.1 Purpose

This test simulates the erosion after a dambreak.

9.2 Description

9.2.1 Physical parameters

The test case of dam failure induces the presence of shock. It allows, among other things, to verify the capacity of the numerical scheme to manage regime changes and to capture shocks. As a general rule, the method using a splitting resolution of the Saint-Venant-Exner system does not allow to ensure the stability of the solution for this type of test case. Considering that this case involves regime changes, the river kernel does not allow to manage this type of configuration and therefore, it will not be tested. The parameters are given in the table 9.1. The final time is $T=1.4$ s.

Channel width	$l =$	0.25	m
Channel length	$L =$	6	m
Gravity constant	$g =$	9.8	m.s^{-2}
Water density	$\rho_w =$	10^3	kg.m^{-3}
Sediment density	$\rho_s =$	2.65×10^3	kg.m^{-3}
Grain diameter	$d =$	3.9×10^{-3}	m
Inflow	$q =$	0	$\text{m}^2.\text{s}^{-1}$
Water depth	$h(x \leq 3) =$	0.35	m
	$h(x > 3) =$	0.01	m
Strickler coefficient	$K_h =$	60	$\text{m}^{1/3}.\text{s}^{-1}$
	$K_s =$	88	$\text{m}^{1/3}.\text{s}^{-1}$
Skin friction Strickler	$K_p =$	20	$\text{m}^{1/3}.\text{s}^{-1}$

Table 9.1: Parameters for the test case of dam failure.

9.2.2 Numerical parameters

The mascaret kernel is used to perform this simulation. The time step is variable respecting a Courant number of 0.8. The mesh size is 0.02 m.

9.3 Results

Figure 9.1 shows the bottom evolution at the beginning and the end of the simulation. Despite some small instabilities, the behavior of the solution corresponds to what is expected.

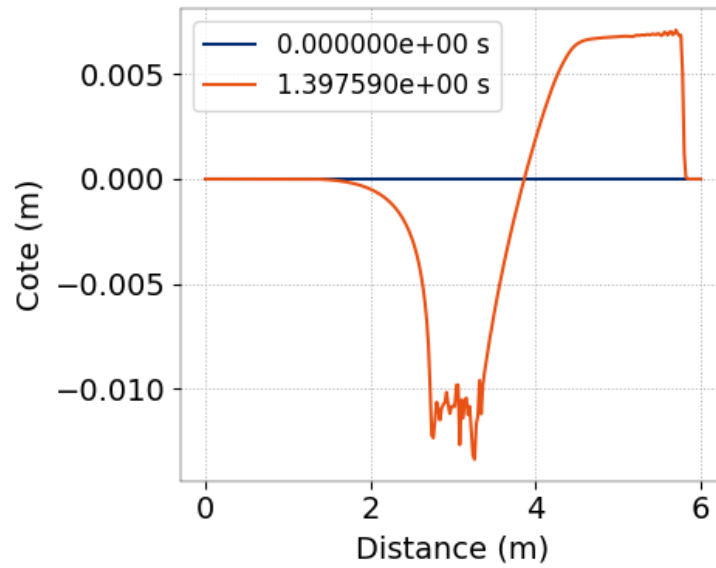


Figure 9.1: Bottom elevation at the initial and final time step.

9.4 Conclusion

COURLIS is able to simulate a dambreak.

- [1] Eugen Meyer-Peter and R Müller. Formulas for bed-load transport. In *IAHSR 2nd meeting, Stockholm, appendix 2*. IAHR, 1948.
- [2] A Recking. Simple method for calculating reach-averaged bed-load transport. *Journal of Hydraulic Engineering*, 139(1):70–75, 2013.
- [3] JP Soni. Laboratory study of aggradation in alluvial channels. *Journal of Hydrology*, 49 (1-2):87–106, 1981.